Point-to-point responses

We appreciate the reviewers for their valuable and constructive comments, which are very helpful for the improvement of the manuscript. We have revised the manuscript carefully according to the reviewers' comments. We have addressed the reviewers' comments on a point-to-point basis as below for consideration, where the reviewers' comments are cited in ***black****, and the responses are in* ***blue****.*

Referee #2

This manuscript presents a high-time resolution dataset of vertical profile of aerosol, NO_2 and HCHO across 32 sites in seven major regions of China from 2019 to 2023, which obtained from the hyperspectral vertical remote sensing network in China. It provides a comprehensive analysis of the patterns of the vertical distribution, seasonal variations and diurnal pattern of these pollutants, and comparisons with the CNEMC stations and the TROPOMI satellite data were conducted and the quality of the present dataset was analyzed. This work is quite challenging, not only because of the complexity of the observation environment, for example, the observation sites include both the Tibetan Plateau and the coastal zone; at the same time, the stability and reliability of the MAX-DOAS work in different observation environments also bring challenges to the data retrievals. Whatever, the good agreement with TROPOMI satellite and ground-based CNEMC measurements showed the data quality is assured.

The dataset it provides could be useful for future scholars in the fields of atmosphere environment and climate change. Overall, this is a good paper that deserves to be published in ESSD. Nevertheless, some minor issues must be clarified.

1) First, the information about the 32 sites is limited, more description should be provided, including the major emission sources around the each site and the site type (urban, suburban, background etc.) and observation period in each site suggested to be added in Table 1. It is important to understand the seasonal and diurnal pattern of the observed pollutants.

Re: Thank you for your valuable comment. We agree that further description and additional details of the sites are necessary. To improve readability, we have included Table S2 in supplement to describe the observation periods for each site. Additionally, Table S1 in supplement provides information on the main emission sources surrounding each site, as well as the site types. We hope these additions will offer a more comprehensive and accessible overview for the readers.

Table S1. The site type and the major emission sources around each site.

No.	Region	Site(code)	Site Type	Major emission sources
1	North China	Chinese Academy of Meteorological Sciences (CAMS)	Urban	Traffic emissions, residential heating, industrial activities
2		The Institute of Atmospheric Physics (IAP)	Urban	Traffic emissions, residential heating, industrial activities
3		Nancheng (NC)	Suburban	Agricultural activities, light industrial emissions
4		University of Chinese Academy of Sciences (UCAS)	Suburban	Traffic emissions, residential heating
5		Wangdu (WD)	Rural	Agricultural activities, biomass burning
6		Xianghe (XH)	Rural	Agricultural activities, biomass burning
7		Shijiazhuang (SJZ)	Urban	Heavy industrial emissions, traffic emissions, residential heating

8		Shanxi University (SXU)	Urban	Industrial emissions, traffic emissions
9		Inner Mongolia Normal University (IMNU)	High-altitude	Dust emissions, agricultural activities
10	East China	Dongying (DY)	Coastal	Oil refineries, petrochemical industries, traffic emissions
11		Qingdao (QD)	Coastal	Ship emissions, industrial activities, traffic emissions
12		Taishan (TS)	High-altitude	Background site, minimal local emissions
13		Tai'an(TA)	Urban	Traffic emissions, industrial activities
14		Shanghai_Xuhui (SH_XH)	Urban	Heavy traffic emissions, industrial activities, residential heating
15		Shanghai_Dianshan Lake (SH_DL)	Lakeside	Traffic emissions, industrial activities, ship emissions
16		Nanjing University of Information Science and Technology (NUIST)	Coastal	Traffic emissions, industrial activities, ship emissions
17		Ningbo (NB)	Coastal	Ship emissions, industrial activities, traffic emissions
18		Huaniao Island (HNI)	Coastal	Ship emissions, minimal local emissions
19		Lin'an(LA)	Rural	Agricultural activities, biomass burning
20		Huaibei Normal University (HNU)	Urban	Industrial emissions, traffic emissions
21		Anhui University (AHU)	Urban	Traffic emissions, industrial activities
22		Changfeng(CF)	Suburban	Traffic emissions, agricultural activities
23	South China	Xiamen_Institute of Urban Environment (IUE)	Urban	Traffic emissions, industrial activities, ship emissions
24		Guangzhou Institute of Geochemistry (GIG)	Urban	Traffic emissions, industrial activities, ship emissions
25		Southern University of Science and Technology (SUST)	Urban	Traffic emissions, industrial activities
26	Southwest China	Shangri-La Station (SLS)	High-altitude	Background site, minimal local emissions
27		Chongqing (CQ)	Urban	Heavy industrial emissions, traffic emissions
28	Northwest China	Lanzhou University (LZU)	Urban	Industrial emissions, traffic emissions, dust storms
29		Xi'an (XA)	Urban	Traffic emissions, industrial activities
30	Northeast China	Juehua Island (JHI)	Coastal	Ship emissions, minimal local emissions
31		Liaoning University (LNU)	Urban	Industrial emissions, traffic emissions
32	Central China	Luoyang (LY)	Urban	Heavy industrial emissions, traffic emissions

Table S2. The site observation period. The months listed in the observation period indicate that the site

has data for a certain month. The specific monthly data integrity is shown in Figure 2.

No.	Region	Site(code)	Observation period	No.	Region	Site(code)	Observation period
1	North China	Chinese Academy of Meteorological Sciences (CAMS)	2019.01-2021.02 2021.04-2021.07 2021.10-2023.10 2021.04-2021.07	17	East China	Ningbo (NB)	2019.11-2020.01 2020.05-2020.06 2020.08-2021.03 2021.05-2021.06 2021.09-2021.09 2021.12-2021.12
2		The Institute of Atmospheric Physics (IAP)	2019.09-2021.03 2021.05-2021.05	18		Huaniao Island (HNI)	2019.04-2019.08 2019.11-2020.07 2020.11-2022.04
3		Nancheng (NC)	2019.01-2020.01 2020.05-2021.03 2021.07-2021.10 2021.12-2022.05	19		Lin'an(LA)	2020.12-2020.12 2021.02-2022.07
4		University of Chinese Academy of Sciences (UCAS)	2019.01-2020.02 2020.06-2021.07 2021.11-2022.07 2022.09-2023.05	20		Huaibei Normal University (HNU)	2020.06-2022.05
5		Wangdu (WD)	2019.03-2023.03 2023.06-2023.12	21		Anhui University (AHU)	2020.12-2023.09
6		Xianghe (XH)	2019.01-2019.01 2019.03-2019.10 2020.01-2021.05 2021.08-2022.01 2022.05-2022.05	22		Changfeng(CF)	2022.05-2022.12 2023.03-2023.12
7		Shijiazhuang (SJZ)	2019.10-2021.03 2021.05-2022.05	23	South China	Xiamen_Institute of Urban Environment (IUE)	2020.01-2020.03 2020.06-2020.09 2021.04-2021.05
8		Shanxi University (SXU)	2020.10-2020.11 2021.04-2022.03 2022.07-2023.07 2023.09-2023.12	24		Guangzhou Institute of Geochemistry (GIG)	2019.09-2021.10 2022.03-2023.11
9		Inner Mongolia Normal University (IMNU)	2020.07-2021.10 2022.01-2022.08 2023.10-2023.10	25		Southern University of Science and Technology (SUST)	2019.01-2021.11 2022.01-2022.12
10	East China	Dongying (DY)	2019.09-2019.09 2019.11-2020.05 2020.10-2021.07	26	Southwest China	Shangri-La Station (SLS)	2019.11-2022.08
11		Qingdao (QD)	2019.12-2020.12	27		Chongqing (CQ)	2019.01-2020.03 2020.05-2023.01 2023.03-2023.04
12		Taishan (TS)	2020.01-2020.02 2020.04-2022.07 2023.03-2023.03	28	Northwest China	Lanzhou University (LZU)	2019.01-2021.11
13		Tai'an(TA)	2021.06-2021.06 2021.08-2021.08 2021.12-2022.01	29		Xi'an (XA)	2020.01-2020.06 2020.08-2020.08
14		Shanghai_Xuhui (SH_XH)	2019.09-2020.01 2020.03-2020.12	30	Northeast China	Juehua Island (JHI)	2020.09-2021.06
15		Shanghai_Dianshan Lake (SH_DL)	2019.01-2019.06	31		Liaoning University (LNU)	2019.07-2019.07 2019.09-2019.12
16		Nanjing University of Information Science and Technology (NUIST)	2019.01-2019.07 2019.09-2019.11 2022.04-2023.12	32	Central China	Luoyang (LY)	2020.02-2022.02

2) Second, as the vertical dataset covers the period of 2019-2023, which significant improvements in air quality and decrease of air pollutants at ground had been reported, it would be interesting to provide the analysis of temporal changes of the observed pollutants (aerosol, NO_2 and HCHO) in the upper atmosphere.

Re: Thanks for your great comments. In response to your suggestion, we have conducted a more detailed

analysis of the temporal changes of pollutants (aerosols, NO_2, and HCHO) observed in the upper atmosphere between 2019 and 2023 and provide a comprehensive response below:

Existing studies indicate that the most severe air pollution in China occurred approximately between 2013 and 2015 (Zheng et al., 2018), followed by significant improvements in air quality since 2017 (Ma et al., 2019). Consequently, while air quality continued to improve during the 2019–2023 period, the rate of improvement may have slowed, entering a plateau phase. This relative stability of pollutant concentrations at the surface level could also contribute to relatively modest changes in pollutant levels in the upper atmosphere.

Against this backdrop, we conducted a time series analysis of aerosol, NO_2, and HCHO concentrations at various sites across different altitude layers from 2019 to 2023. As described in the manuscript, we used the 0-100m, 500-600m, and 900-1000m layers to represent the lower, middle, and upper boundary layers, respectively. The results indicate that the overall trends of the three pollutants in the upper atmosphere are generally consistent with those in the middle and lower layers. However, at certain sites and during specific periods, the trends in the lower layers may deviate from those in the middle and upper layers. Notably, interannual variations in pollutant concentrations are less pronounced in the upper atmosphere, whereas seasonal variations and diurnal patterns are more evident. Furthermore, the concentration fluctuations in the lower layers of the three pollutants are significantly greater than those in the middle and upper layers, and their concentration levels differ notably from those in the upper layers, with the most noticeable differences observed in the NO_2 time series. To quantify these differences, we calculated the ratios of average concentrations between altitude layers. For aerosols, the ratio of aerosol extinction coefficient in the upper layer to that in the lower layer is 33.09%, while the ratio in the middle layer to the lower layer is 64.36%. For NO_2, these values are 15.29% and 32.98%, respectively, while for HCHO, the corresponding ratios are 56.36% and 80.88%. Among the three pollutants, HCHO exhibits the smallest vertical gradient, indicating that its concentration differences and fluctuations across the lower, middle, and upper layers are relatively minimal. This suggests a more uniform vertical distribution of HCHO compared to aerosols and NO_2.

We have plotted the time series in Figures S1-S3 and added the relevant explanatory content in line 178 and Section S2, as follows:

Line 178, “The time series of aerosol extinction coefficient, NO_2 concentration, and HCHO concentration for the three altitude layers during 2019–2023 are shown in Figures S1-S3, with the corresponding correlation analysis provided in Section S2.”

Section S2, “Figures S1–S3 display the time series of aerosol extinction coefficient, NO_2 concentration, and HCHO concentration in the lower, middle, and upper layers between 2019 and 2023. The results indicate that the overall trends of the three pollutants in the upper atmosphere are generally consistent with those in the middle and lower layers. However, at certain sites and during specific periods, the trends in the lower layers may deviate from those in the middle and upper layers. Notably, interannual variations in pollutant concentrations are less pronounced in the upper atmosphere, whereas seasonal variations and diurnal patterns are more evident. Furthermore, the concentration fluctuations in the lower layers of the three pollutants are significantly greater than those in the middle and upper layers, and their concentration levels differ notably from those in the upper layers, with the most noticeable differences observed in the NO_2 time series. To quantify these differences, we calculated the ratios of average concentrations between altitude layers. For aerosols, the ratio of aerosol extinction coefficient in the upper layer to that in the lower layer is 33.09%, while the ratio in the middle layer to the lower layer is 64.36%. For NO_2, these values are 15.29% and 32.98%, respectively, while for HCHO, the corresponding ratios are 56.36% and 80.88%. Among the three pollutants, HCHO exhibits the smallest vertical gradient, indicating that its concentration differences and fluctuations across the lower, middle, and upper layers are relatively minimal. This suggests a more uniform vertical distribution of HCHO compared to aerosols and NO_2.”

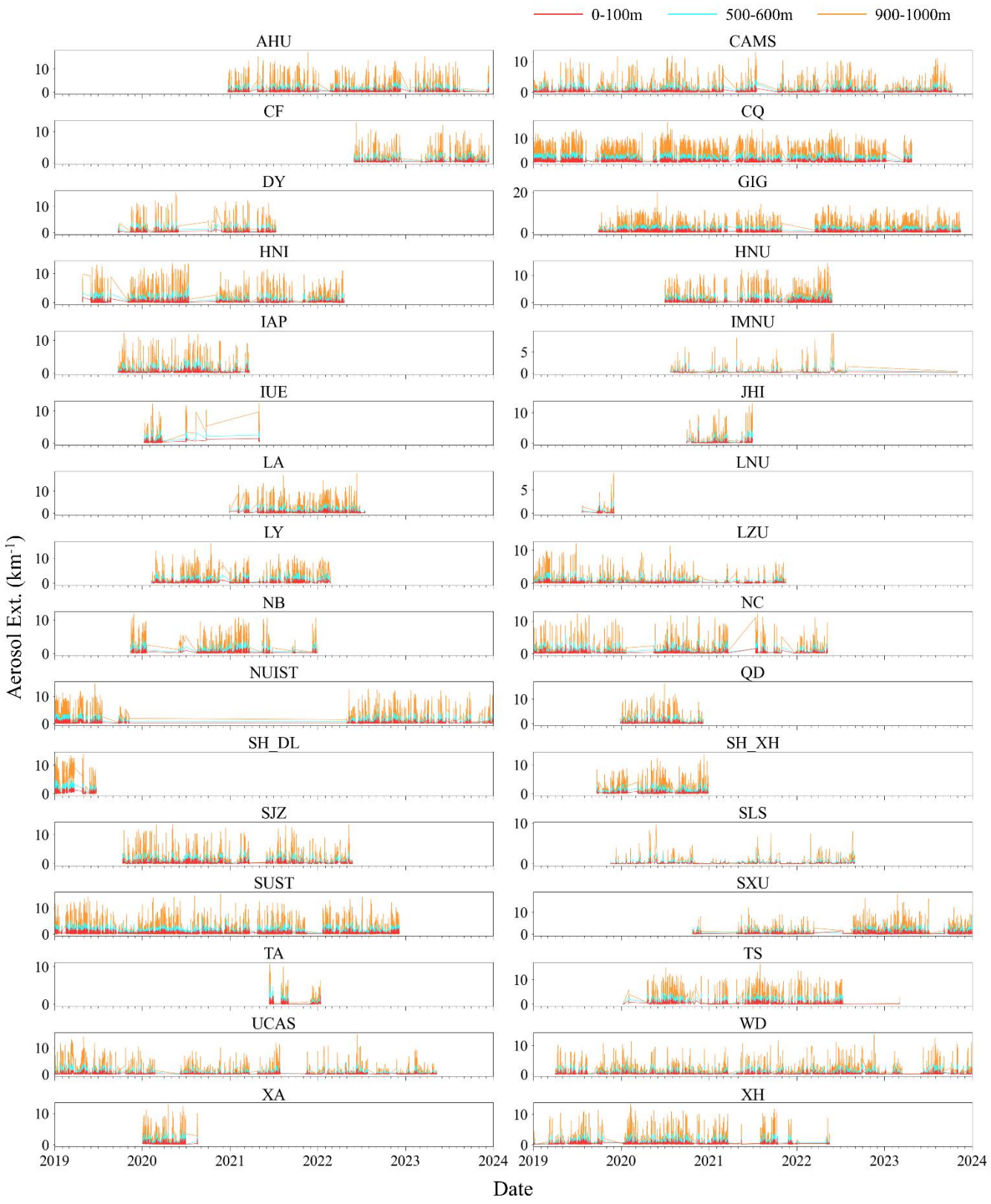

Figure S1. Time series of aerosol extinction during 2019-2023.

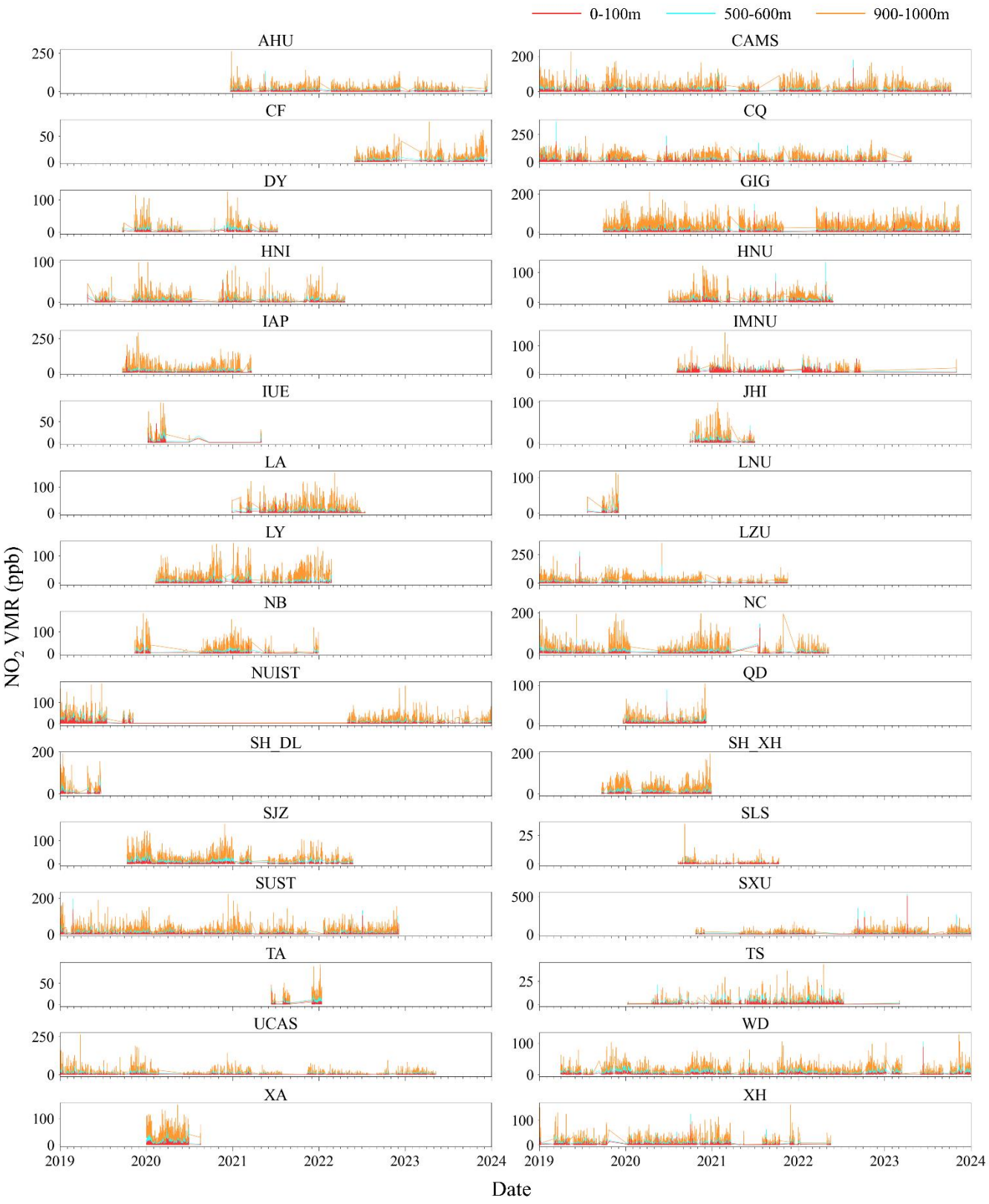

Figure S2. Time series of NO_2 concentration during 2019-2023.

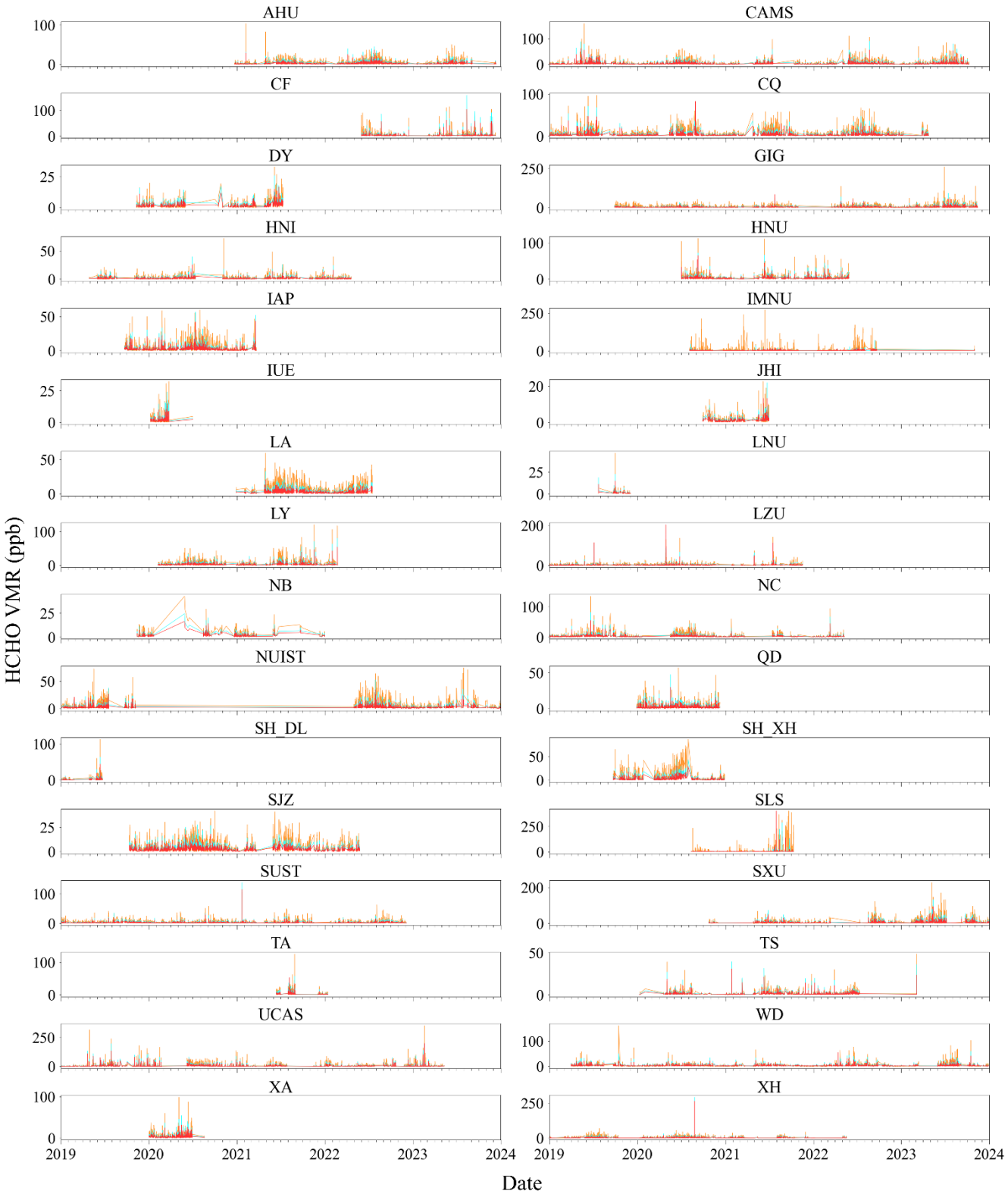

Figure S3. Time series of HCHO concentration during 2019-2023.

3) Finally, discussion about the diurnal pattern of HCHO should be re-examined. For example, the evening peak of HCHO at the UCAS site was much enhanced than the IAP site (Figure 10), apparently, it could not be due to vehicular emissions during evening rush hours, as the former received much more traffic emissions (Figure 8).

Re: We sincerely appreciate your insightful comments, which have drawn our attention to this

phenomenon. The explanation for the observed evening peak of HCHO at the UCAS site is as follows: The UCAS site is located in a suburban area with relatively high vegetation coverage, leading to substantial emissions of volatile organic compounds (VOCs). Through photochemical reactions, VOCs contribute to the formation of HCHO, leading to its concentration accumulation over time (Nussbaumer et al., 2021). In the late afternoon (16:00–18:00), solar radiation weakens, leading to a reduction in HCHO photolysis and a decrease in its consumption rate (Biswas et al., 2020). Simultaneously, the lowering of the boundary layer height restricts pollutant dispersion, further contributing to the peak in HCHO concentration.

In response to your comment, we have revised the section discussing the diurnal pattern of HCHO. The updated content is as follows:

Line 327, "From 17:00 BJT, HCHO concentrations begin to rise again, peaking at 18:00 BJT, likely due to the lowering of the boundary layer (Franco et al., 2016). At certain suburban and rural sites, high vegetation coverage leads to substantial emissions of volatile organic compounds (VOCs) (Cao et al., 2022), which undergo photochemical reactions to produce HCHO, resulting in its accumulation over time (Nussbaumer et al., 2021). In the evening, the weakening of HCHO photolysis reduces its consumption, combined with the decrease in boundary layer height that limits dispersion, further enhances the concentration peak (Biswas et al., 2020)."

References

Biswas, M. S., Pandithurai, G., Aslam, M. Y., Patil, R. D., Anilkumar, V., Dudhambe, S. D., Lerot, C., De Smedt, I., Van Roozendael, M., and Mahajan, A. S.: Effect of Boundary Layer Evolution on Nitrogen Dioxide (NO2) and Formaldehyde (HCHO) Concentrations at a High-altitude Observatory in Western India, Aerosol Air Qual. Res., 21, 200193, https://doi.org/10.4209/aaqr.2020.05.0193, 2020.

Cao, J., Situ, S., Hao, Y., Xie, S., and Li, L.: Enhanced summertime ozone and SOA from biogenic volatile organic compound (BVOC) emissions due to vegetation biomass variability during 1981–2018 in China, Atmospheric Chemistry and Physics, 22, 2351–2364, https://doi.org/10.5194/acp-22-2351-2022, 2022.

Franco, B., Marais, E. A., Bovy, B., Bader, W., Lejeune, B., Roland, G., Servais, C., and Mahieu, E.: Diurnal cycle and multi-decadal trend of formaldehyde in the remote atmosphere near 46° N, Atmospheric Chemistry and Physics, 16, 4171–4189, https://doi.org/10.5194/acp-16-4171-2016, 2016.

Ma, Z., Liu, R., Liu, Y., and Bi, J.: Effects of air pollution control policies on $PM_{2.5}$ pollution improvement in China from 2005 to 2017: a satellite-based perspective, Atmospheric Chemistry and Physics, 19, 6861–6877, https://doi.org/10.5194/acp-19-6861-2019, 2019.

Nussbaumer, C. M., Crowley, J. N., Schuladen, J., Williams, J., Hafermann, S., Reiffs, A., Axinte, R., Harder, H., Ernest, C., Novelli, A., Sala, K., Martinez, M., Mallik, C., Tomsche, L., Plass-Dülmer, C., Bohn, B., Lelieveld, J., and Fischer, H.: Measurement report: Photochemical production and loss rates of formaldehyde and ozone across Europe, Atmospheric Chemistry and Physics, 21, 18413–18432, https://doi.org/10.5194/acp-21-18413-2021, 2021.

Zheng, B., Tong, D., Li, M., Liu, F., Hong, C., Geng, G., Li, H., Li, X., Peng, L., Qi, J., Yan, L., Zhang, Y., Zhao, H., Zheng, Y., He, K., and Zhang, Q.: Trends in China's anthropogenic emissions since 2010 as the consequence of clean air actions, Atmospheric Chemistry and Physics, 18, 14095–14111, https://doi.org/10.5194/acp-18-14095-2018, 2018.